

Groundwater salinity patterns along the coast of the Western Netherlands and the application of cone penetration tests

Pauw, P. S.; Groen, J.; Groen, M. M.A.; van der Made, K. J.; Stuyfzand, P. J.; Post, V. E.A.

DOI

[10.1016/j.jhydrol.2017.04.021](https://doi.org/10.1016/j.jhydrol.2017.04.021)

Publication date

2017

Document Version

Final published version

Published in

Journal of Hydrology

Citation (APA)

Pauw, P. S., Groen, J., Groen, M. M. A., van der Made, K. J., Stuyfzand, P. J., & Post, V. E. A. (2017). Groundwater salinity patterns along the coast of the Western Netherlands and the application of cone penetration tests. *Journal of Hydrology*, 551, 756-767. <https://doi.org/10.1016/j.jhydrol.2017.04.021>

Important note

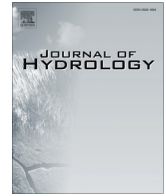
To cite this publication, please use the final published version (if applicable). Please check the document version above.

Copyright

Other than for strictly personal use, it is not permitted to download, forward or distribute the text or part of it, without the consent of the author(s) and/or copyright holder(s), unless the work is under an open content license such as Creative Commons.

Takedown policy

Please contact us and provide details if you believe this document breaches copyrights. We will remove access to the work immediately and investigate your claim.



Research papers

Groundwater salinity patterns along the coast of the Western Netherlands and the application of cone penetration tests



P.S. Pauw^{a,*}, J. Groen^b, M.M.A. Groen^b, K.J. van der Made^c, P.J. Stuyfzand^{d,e}, V.E.A. Post^f

^a Deltares, Unit Subsurface and Groundwater Systems, PO Box 85467, 3508 AL Utrecht, The Netherlands

^b Acacia Water, Van Hogendorpplein 4, 2805 BM Gouda, The Netherlands

^c Wiertsema en Partners, Feithspark 6, 9356 BZ Tolbert, The Netherlands

^d TU Delft, Faculty of Civil Engineering and Geosciences, Stevinweg 1, PO Box 5048, 2628 CN Delft/2600 GA Delft, The Netherlands

^e KWR, KWR Watercycle Research Institute, PO Box 1072, 3430 BB Nieuwegein, The Netherlands

^f BGR, Federal Institute for Geosciences and Natural Resources (BGR), Stilleweg 2, 30655 Hannover, Germany

ARTICLE INFO

Article history:

Available online 12 April 2017

Keywords:

Saltwater intrusion
Submarine groundwater discharge
Offshore fresh groundwater
Cone penetration tests

ABSTRACT

Submarine groundwater discharge is an important part of the hydrological cycle, but remains under-investigated for confined aquifers with no surface outcrop at the beach. This paper considers the offshore directed flow of fresh groundwater in the unconfined and confined aquifers along the coast of the Western Netherlands. Salinity patterns based on hydrological, geological, and geophysical field data are presented in five shore-normal hydrogeological cross-sections, extending from the beach to 4 km inland. The offshore continuation of the fresh groundwater is discussed using analytical models and cone penetration tests (CPTs) performed at the beach. All CPTs taken around the low water line of the intertidal zone reveal that changes from saline to fresh groundwater are always associated with a low-permeable layer. Such a low-permeable layer, which can be as thin as a few decimetres, may form the confining layer between the unconfined and confined aquifers, or can occur within the unconfined aquifer. Due to its high vertical resolution, a CPT is an effective method to detect these variations in salinity and lithology. At each of the investigated locations, freshwater was present in the confined aquifer. Assuming that this fresh groundwater is part of an active flow system, the submarine freshwater tongue is estimated to extend at least a few hundred meters offshore, based on analytical model calculations. Hydrochemical data from an old offshore borehole, however, suggest this may be an underestimate and that the submarine freshwater tongue originates from former times when the coastline was located further westward than nowadays.

© 2017 Elsevier B.V. All rights reserved.

1. Introduction

Aquifers in coastal areas contain freshwater reserves that are vital to sustain human populations and ecosystems. Understanding the salinity distribution and groundwater flow patterns at the coast is important when investigating saltwater intrusion (Custodio and Bruggeman, 1987; Bear et al., 1999), as well as submarine groundwater discharge (Taniguchi et al., 2002; Moore, 2010). Moreover, this understanding is also crucial when adopting boundary conditions of mathematical groundwater models (Bakker and Schaars, 2006), which are widely used for the manage-

ment of coastal freshwater resources (Bear et al., 1999; Werner et al., 2013).

Most of the submarine groundwater discharge studies published to date focus on shallow, unconfined aquifers and have yielded valuable insights on a number of well-characterised study sites, including De Panne, Belgium (Lebbe, 1983; Vandenbohede and Lebbe, 2005), Waquoit Bay, USA (Michael et al., 2005; Mulligan and Charette, 2006; Abarca et al., 2013), and Queensland, Australia (Robinson et al., 2007). Based on field measurements and numerical modelling, these investigations demonstrated the existence of a brackish-saline groundwater circulation cell below the beach. This circulation cell is primarily driven by the infiltration of seawater during rising tide and the discharge of groundwater (seepage) during falling tide. Inland-derived fresh groundwater may flow below this circulation cell, mix with the infiltrated seawater, and discharge at the lower part of the beach. Factors that influence the flow patterns and salinity variations include the mor-

* Corresponding author.

E-mail addresses: pieter.pauw@deltares.nl (P.S. Pauw), koos.groen@acaciawater.com (J. Groen), michel.groen@acaciawater.com (M.M.A. Groen), c.made@wiersema.nl (K.J. van der Made), p.j.stuyfzand@tudelft.nl, pieter.stuyfzand@kwrwater.nl (P.J. Stuyfzand), vincent.post@bgr.de (V.E.A. Post).

phology of the beach, the tidal regime, wave action, and the flux of fresh groundwater that discharges offshore (Michael et al., 2005; Robinson et al., 2007; Abarca et al., 2013; Greskowiak, 2014).

In contrast to superficial, unconfined aquifers, considerably fewer studies of submarine groundwater discharge have focused on confined aquifers. Confined aquifers that extend offshore fundamentally differ from unconfined aquifers in that fresh groundwater continues to flow below the seabed instead of terminating near the shore, giving rise to an offshore tongue of fresh groundwater. This tongue can extend many kilometres below the seabed, and its length depends on the freshwater flux, the permeability of the confined aquifer and the confining layer, and the horizontal extent of the confining layer (Kooi and Groen, 2001; Bakker, 2006).

Because direct observation in the offshore region is more difficult, more expensive and has traditionally been considered less relevant than onshore investigations, very few observations exist in aquifers below the seabed. A geophysical study in Indian River Bay, USA, showed that freshwater occurs up to 1 km offshore where layers of silt and peat prevent seawater from intruding into a sandy aquifer (Krantz et al., 2004). The significance of palaeochannels was demonstrated by Mulligan et al. (2007) who used field data and numerical modelling at a field site in North Carolina, USA, to show that where these channels breach an offshore confining layer, seawater can intrude along the channel axis, while brackish groundwater discharges along the channel margins. Heterogeneity can also influence the offshore flow of fresh groundwater on a local scale, as was shown by Andersen et al. (2007) in their study near the coast of Esbjerg, Denmark. These studies have highlighted the important role of the lithological variability on groundwater flow and salinity patterns, and the need of detailed field studies to understand these interactions.

The objective of this paper is to provide enhanced understanding of offshore and nearshore salinity patterns in layered unconfined-confined aquifer systems. To this end, salinity patterns were analysed in shore-normal hydrogeological cross-sections along the western coast of the Netherlands, extending from the beach to 4 km inland. The coastal dune belt is of critical importance to the potable water supply in the Netherlands. While a wealth of onshore data is available with data from as early as 1900, flow conditions on the seaward side remain poorly understood due to a lack of observations offshore or close to the shoreline. Existing data were therefore complemented by conducting cone penetration tests (CPTs) at the beach. The CPTs penetrated into the unconfined, as well as into the confined aquifer. The CPT measurements provide information about the variation of the lithology and resistivity, which is a proxy for groundwater salinity, at a vertical resolution of 2 cm (Lunne et al., 1997). By analysing the relationship between small-scale heterogeneity and salinity at this scale, it is demonstrated how this technique can be useful in future studies of coastal (beach) hydrology. While the collected data also provide information about the unconfined aquifer, they are not sufficient to unambiguously delineate the saline circulation cell that has been identified in the aforementioned studies of SGD in unconfined aquifers. The analysis presented in this article therefore focuses primarily on the confined aquifer.

2. Material and methods

2.1. Study area

Fig. 1 shows a representative schematic shore normal cross-section of the fresh dune groundwater flow system of the Western Netherlands, where the width of the dune area varies between 1 and 8 km. The climate is of the maritime temperate type according to the Köppen climate classification system. The natural recharge

rate in the dune area ranges between 210 and 620 mm yr⁻¹ and is strongly related to vegetation type (Stuyfzand, 1993). Groundwater flows towards the North Sea in the west and to the low lying polder area in the east (Stuyfzand, 1993).

The current groundwater salinity distribution below and in the vicinity of the dune area is the result of a sequence of historical processes. Between 3800 BCE and 1000 CE, a system of barrier islands developed along the coast of the Western Netherlands. Below individual small-scale dune systems on these islands (the “Old Dunes”), shallow freshwater lenses developed in the brackish/saline subsurface. From around 1000 CE, marine erosion resulted in an eastward shift of the coastline, and dissected the low-lying Old Dunes landscape. A new generation of dunes (the “Young Dunes”) formed from this time onward, and covered most of the Old Dune remnants, leading to a much wider and higher coastal dune belt. As the width of the coastal dune belt expanded, so did the freshwater lens below it.

Between approximately 1000 CE and 1200 CE man started to exploit and drain the wetlands and salt marshes landward of the dune area. Later, from 1550 CE till the end of the 19th century several large lakes inland of the dune belt were reclaimed. These processes led to widespread land subsidence and a concomitant lowering of surface water levels and water tables, which reached several meters in some areas and is ongoing. Consequently, much of the groundwater flow in the freshwater lens below the dunes was deflected eastward, and intrusion of North Sea water was induced via deep flow paths underneath the freshwater lens (Stuyfzand, 2016).

In 1853 surface water and groundwater exploitation began in the dune area. Until the beginning of 20th century, groundwater exploitation took place in the upper, unconfined aquifer. From 1903 onward also the confined aquifer was exploited. The exploitation led to severe saltwater intrusion and a decline of the thickness of the freshwater lens up to several tens of meters locally (Stuyfzand, 1993). From 1955 artificial recharge projects were started in the dunes. First, river water was infiltrated using spreading basins. Since 1990, deep well injection was applied in the confined aquifers. Presently, the artificial recharge has nearly restored the original volume of the freshwater lens.

The focus in the study area is on five shore-normal hydrogeological cross-sections (Fig. 2). The cross-sections are indicated by a number (e.g., ‘42’, the numbers correspond to marker poles on the beach). They are 4 km wide and extend from inland in the dune area (east) to the beach (west). In Fig. 3, the aquifers and aquitards, topography, and groundwater salinity distribution at each of the five cross-sections are shown. The hydrogeological units in Fig. 3 are adopted from extensive studies by Stuyfzand (1985, 1987a,b, 1993), and Stuyfzand et al. (1993), and were constructed based geophysical data, hydrochemical analysis of the groundwater, and on manual interpolation between boreholes. The deepest part of the freshwater lens varies between –50 m and –110 m NAP among the transects. The upper 150 m of the subsurface below the dunes consists of unconsolidated eolian, fluvial, marine, glacial, and periglacial deposits of Quaternary age. Three sandy aquifers are generally distinguished, which are separated by confining layers composed of peat, clay, loam, or glacial till. The continuity and thickness of these confining units varies, which results in different degrees of connectivity between the aquifers.

The average tidal amplitude is about 0.8 m. During spring and neap tide, the tidal amplitude is about 0.2 m higher and 0.1 m lower, respectively. Storms can elevate the sea level by up to a few meters. The average slope of the intertidal area (i.e., the beach area between the lowest and highest astronomical tide mark) varies between 0.025 and 0.04.

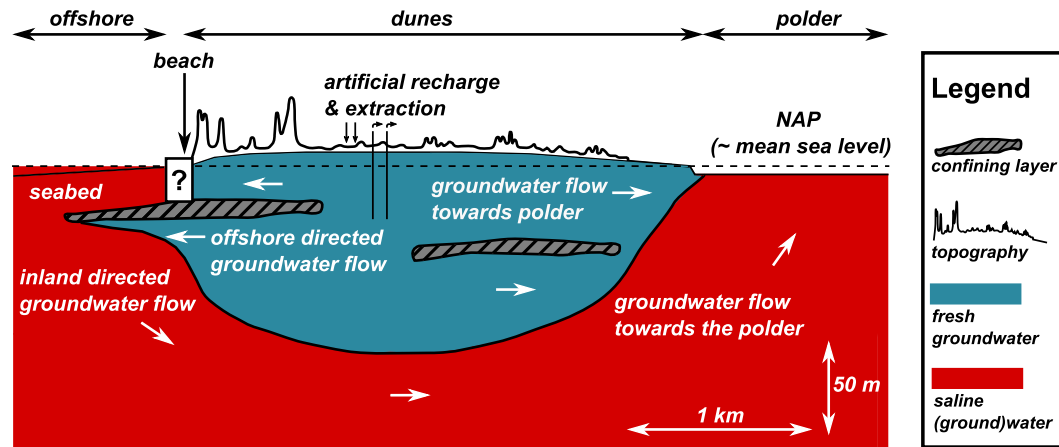


Fig. 1. Conceptual shore-perpendicular cross section of the fresh groundwater flow system below the coastal dunes of the Western Netherlands, including a concept of the offshore continuation of fresh groundwater flow system. The boxed question mark indicates the unknown groundwater salinity distribution below the beach and the nearshore region. The offshore tongue of fresh groundwater is a premise rather than a data-supported feature.

2.2. Cone penetration tests (CPTs)

At the most seaward (western) point of each cross-section, a measurement location (ML) is located on the beach where two CPTs were conducted; one at the lower (seaward) part of the beach (indicated by 'L'), and the other (indicated by 'H') at a higher part of the beach, 50–100 m inland of 'L' (Table 1). During the CPTs, a probe with a conical tip (Fig. 4) is pushed into the subsurface by a heavy truck. The penetration rate used in this study was circa 2 cm s^{-1} . Each 2 cm the cone resistance, sleeve friction, water pressure, and the bulk electrical resistivity were measured (Lunne et al., 1997). The cone resistance (q_c) [$\text{M L}^{-1} \text{T}^{-2}$] is the force acting on the cone divided by the cone surface area and is measured at the tip of the probe (Fig. 4). Along the sides of the probe, the sleeve friction (f_s) [$\text{M L}^{-1} \text{T}^{-2}$] is measured. The sleeve friction is the horizontal force on the sleeve per unit surface area, and is a measure of the cohesiveness of the penetrated material. The water pressure (u) [$\text{M L}^{-1} \text{T}^{-2}$] is measured at or just behind the cone. The bulk electrical resistivity ρ_b [$\text{M L T}^{-3} \text{I}^{-2}$] is measured above the friction sleeve using electrodes, separated by electrically insulating material.

Fine grained layers can be detected using the friction ratio (R_f in %). R_f is defined as:

$$R_f = \frac{f_s}{q_c} \cdot 100 \quad (1)$$

Values of the friction ratio $R_f > 1.8$ were used to identify fine grained layers. This value was chosen based on visual inspection of strong anomalies in the change of the R_f values with depth. In addition, and in a similar way, anomalies in the vertical gradient of the measured water pressure u was used to identify layers of low permeability. A change of u (du) per unit change in depth (dz) $|\frac{du}{dz}| > 2.0 \cdot 10^7 \text{ Pa m}^{-1}$ was selected as a threshold value.

In the Electronic Supplement of this paper, where the raw values of q_c , f_s , R_f , u , and ρ_b are presented for each of the CPTs, it can be seen that anomalies in R_f generally correspond with anomalies in u . At MLs 91 and 94 fine-grained layers could only be identified based on R_f as u was not measured here. More detailed information about the measurement of q_c , f_s , u , ρ_b , in particular regarding the methods to classify the lithology based on these parameters, can be found in Lunne et al. (1997). The work presented in the present paper focussed on inferring the groundwater salinity from ρ_b and on distinguishing fine grained, low permeable layers from coarser layers using the aforementioned indicators.

A green horizontal line was used to indicate a fine-grained layer (see Fig. 6 in Section 3). The resolution was 2 cm, thus consecutive green lines form green bands that indicate thick, fine-grained units. No information on the absolute values of the permeability of the fine-grained layers was collected, but since they are known to have a lower hydraulic conductivity than the coarse-grained units, the fine-grained layers are denoted as 'low permeable layers' in the remainder of this paper.

The groundwater salinity was inferred from the measured bulk electrical resistivity ρ_b [$\text{M L}^3 \text{T}^{-3} \text{I}^{-2}$] (i.e., the electrical resistivity due to both groundwater and sediment). ρ_b was related to the electrical resistivity of groundwater (ρ_w) [$\text{M L}^3 \text{T}^{-3} \text{I}^{-2}$] by (Archie, 1942):

$$\rho_b = F \rho_w \quad (2)$$

This relationship assumes that the sediment or rock matrix has an infinite electrical resistivity. F is the formation factor, which was defined by Archie (1942) as:

$$F = n^{-m}, \quad (3)$$

with n being the porosity and m the so-called cementation exponent. For unconsolidated sediment, the cementation component is on average 1.3 (Archie, 1942). This value was also adopted here.

The following empirical relationships were used to relate R_f to F (van den Helder, 2011):

$$\begin{aligned} &\text{if } R_f \leq 3.0 : \\ &F = -2.238 \ln(R_f) + 4.3521 \\ &\text{else :} \\ &F = -1.223 \ln(R_f) + 3.4128 \end{aligned} \quad (4)$$

Eq. (4) was derived from measured groundwater resistivity, bulk resistivity, and R_f values at various locations in the coastal zone of the Netherlands. Although this empirical relationship is representative for the unconsolidated sediments in the study area, it was not thoroughly validated at the MLs. For this reason, an uncertainty indication is also given by using the lower and upper estimated values of the formation factor in case the sediments have a negligible clay content (so that it can be assumed that the sediment has an infinite electrical resistivity compared to that of the groundwater). The minimum and maximum formation factor were constrained based on porosity data from Walter (1976) and Dufour (1998). For the minimum porosity value of 0.25 (poorly

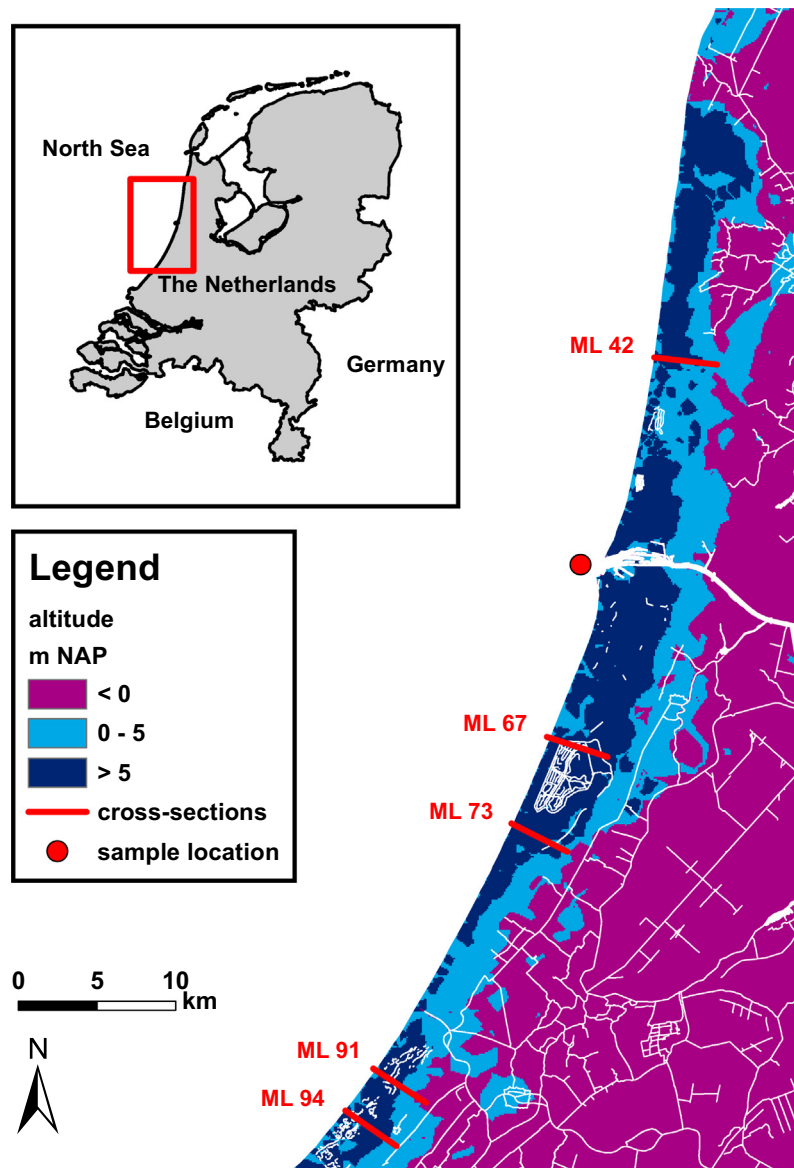


Fig. 2. Map of the study area, with the measurement locations (MLs), the hydrogeological cross-sections (Fig. 3), and surface elevation. Surface water features, including the infiltration ponds for artificial infiltration in the dunes, are indicated by white lines. The red dot indicates the location where groundwater samples were taken approximately 2 km offshore in 1964 (see Section 4). (For interpretation of the references to colour in this figure legend, the reader is referred to the web version of this article.)

sorted, coarse sand) and for the maximum value of 0.45 (fine sand), the corresponding values of F according to Eq. (3) are 2.8 and 6.1, respectively.

When the sediment has considerable clay content, Eq. (3) cannot be used to determine F because the electrical double layer that is present at the interface between the clay particles and the water conducts part of the electrical current (Waxman and Smits, 1968). Methods to determine ρ_w from ρ_b that account for this exist (Revil et al., 2012), but require additional data, such as the cation exchange capacity of the sample. This data was not available in this study, and moreover, may vary considerably over short distances depending on the mineralogy and grain size of the sediment. Therefore, although Eqs. (2)–(4) are used to convert bulk resistivity ρ_b to water resistivity ρ_w , the calculated ρ_w in low-permeable layers (identified using R_f and u) is associated with a high uncertainty.

The salinity of groundwater is proportional to electrical conductivity, and hence, inversely proportional to the (calculated) ρ_w . Indicative values of ρ_w in terms of groundwater salinity that were used here are: fresh water: $\rho_w > 5 \Omega\text{m}$ and saline water $\rho_w <$

$\leq 5 \Omega\text{m}$. ρ_w also depends on temperature. Subsurface temperatures cannot be measured accurately during a CPT due to the heating of the probe caused by friction as it moves into the sediment. Temperature differences due to lateral variability between the sites, depth and seasonal influences are not expected to exceed 5°C , and therefore, the uncertainty imparted on the estimated values of ρ_w is less than 10% (Hayashi, 2003), which is much lower than the uncertainty related to F .

2.3. Continuous vertical electrical soundings

At ML 42, continuous vertical electrical sounding (CVES) measurements were performed to obtain the spatial distribution of ρ_b along a vertical, two-dimensional cross section. The ABEM Lund Imaging System, consisting of the ABEM SAS 4000 terrameter and the ES10-64 electrode selector, was used. The Wenner configuration was applied for all CVES measurements. The apparent resistivity measurements were interpreted using the RES2DINV program (Loke, 2006).

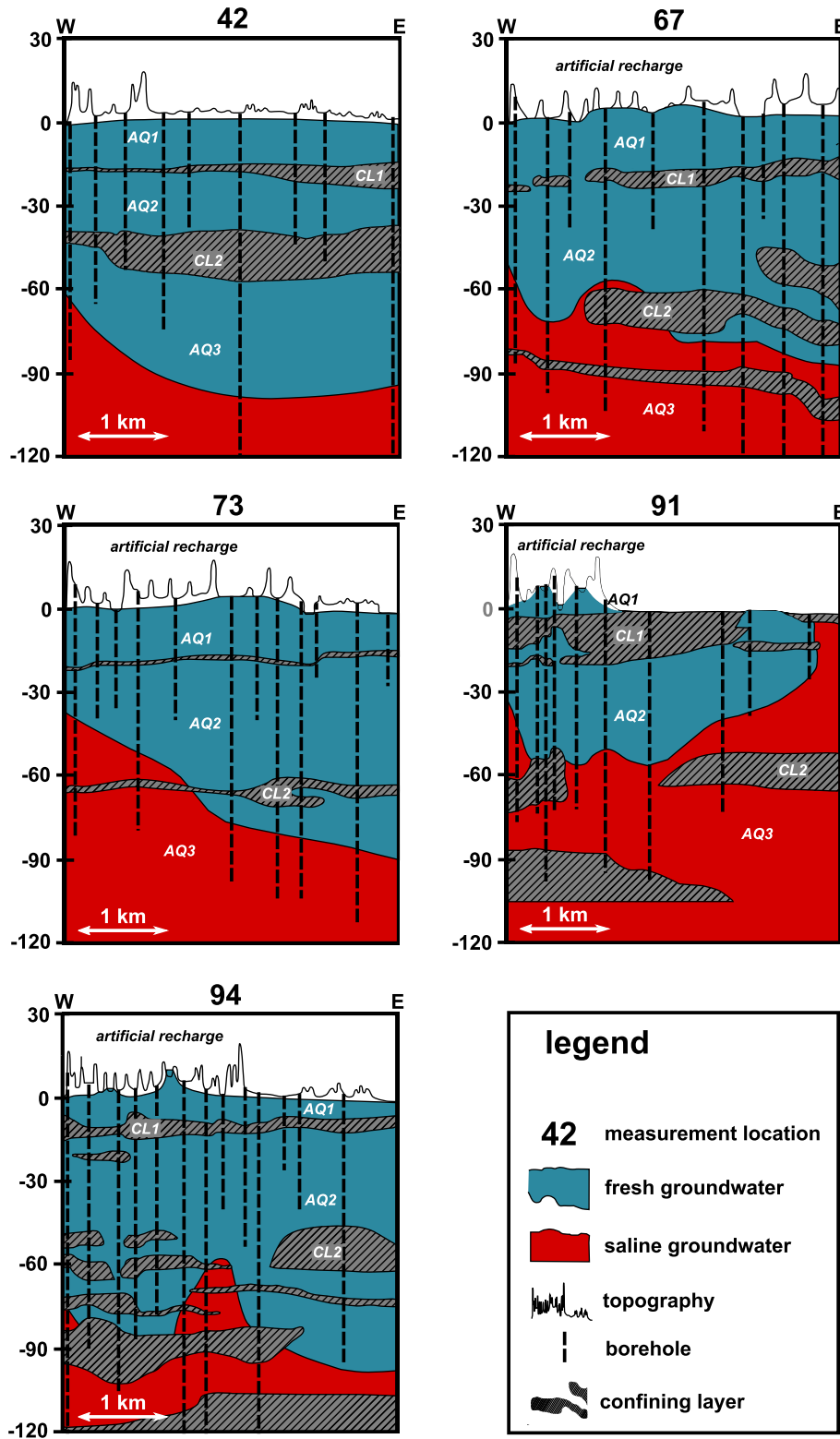


Fig. 3. Shore-perpendicular cross-sections of the groundwater salinity distribution and the main aquifers and confining layers (AQ n and CF n , respectively, with n being the number of the aquifer or confining layer), inland of each ML. The location of these transects is shown in map view in Fig. 2. The numbers next to the vertical axes indicate the depth relative to NAP (approximately mean sea level). 'Fresh' refers to groundwater with a chloride concentration <300 mg l⁻¹, whereas a higher chloride concentration is indicated by 'saline' (based on Stuyfzand (1993)).

Three CVES measurements were conducted (Fig. 5). CVES A-A' was performed at the beach, along the CPTs 42L and 42H using an electrode distance of 1 m, resulting in a profile length of 80 m. CVES B-B' was oriented parallel to the shoreline, at the lower part

of the beach. An electrode distance of 5 meters was used, resulting in a profile length of 400 m. CVES C-C' was done offshore, using a marine cable lying on the seabed, approximately in line with CVES A-A' onshore, with the most landward electrode within 100 m from

Table 1
Horizontal distance between CPT measurements 'L' and 'H' and their elevations.

ML	Horizontal distance 'H'-'L' (m)	Elevation 'H' (m NAP)	Elevation 'L' (m NAP)
42	81	2.22	-0.03
67	112	5.74	-0.44
73	96	3.58	-0.4
91	53	0.44	-0.91
94	89	2.92	-0.3

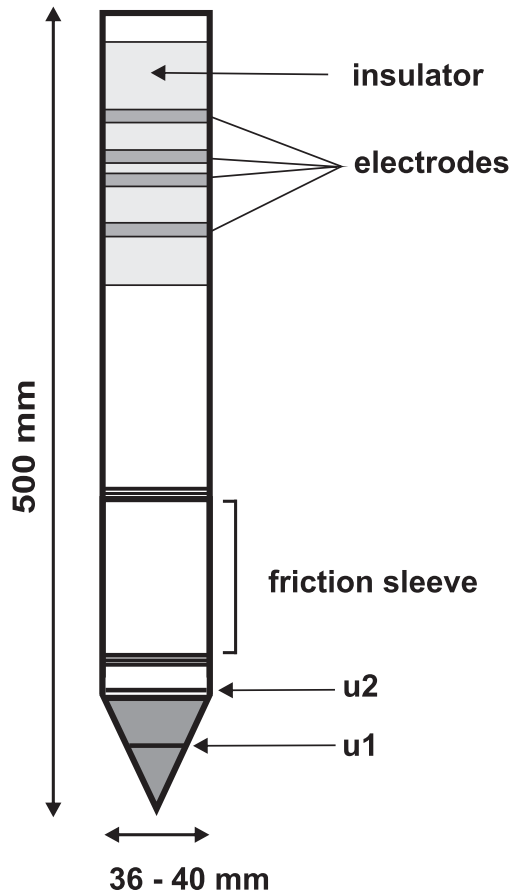


Fig. 4. Sketch of the probe that is pushed into the subsurface during a CPT. At ML 42 only two electrodes were used to measure the bulk resistivity, and the water pressure was measured at u2. At the other MLs, four electrodes were used, and the water pressure was measured at u1.

the lower part of intertidal area. The electrode distance was 5 m, resulting in an offshore profile length of 400 m.

2.4. Offshore continuation of the dune groundwater flow system

While the presence of freshwater at the location of the CPTs near the low-water line can be taken as an indication of the continuation of the fresh groundwater offshore, it does not indicate how far the freshwater extends. Therefore, the analytical solutions presented by Bakker (2006) were used as a first assessment tool to calculate the length of the tongue of fresh groundwater (L [L]) in the confined aquifer (AQ2, see Fig. 3) below the seabed. The most important assumptions of the equations of Bakker (2006) are: 1) the fresh and saline groundwater are immiscible fluids with different but uniform densities, 2) the Dupuit assumption is valid, 3) the flow parallel to the shoreline is negligible, 4) the groundwater flow system is at steady state, and 5) the flow is confined in the onshore

region (uniform horizontal groundwater flow) and semi-confined (horizontal groundwater flow in the aquifer and upward flow of fresh groundwater through a leaky layer) in the offshore region. Furthermore, it is assumed that saltwater fingering (free convection) does not occur. The appropriateness of these assumptions will be elaborated in Section 4.

For brevity, the equations of Bakker (2006) are presented in the Electronic Supplement of this paper. The equations require six input parameters: the (constant) thickness of the confined aquifer H [L], the vertically integrated groundwater flow in the confined section per unit length parallel to the shoreline Q [$L^2 T^{-1}$], the hydraulic conductivity k [$L^{-1} T^{-1}$] of the confined aquifer, the hydraulic resistance of the semi-confining layer c [T], and the densities [$M L^{-3}$] of fresh ρ_f and saline ρ_s groundwater. The length of the semi-confining layer extending offshore L_s [L] was chosen to be far enough to accommodate the full length of the offshore tongue of fresh groundwater (cases I and II in Bakker (2006)), because on the extent of L_s was not available in this study. The values of Q , H , c , and k at the five hydrogeological cross-sections were estimated based on data presented in Stuyfzand (1985, 1987a) and Stuyfzand et al. (1993), and are shown in Table 2. The hydraulic resistance c of the confining layer at cross-sections 67 and 73 could not be determined from literature. Instead, the value of c was found by adjusting its value in the equations of Bakker (2006) until the calculated and measured thicknesses of the freshwater lens at the lower part of the beach (inferred from CPTs 67L and 73L) matched. Q was determined based on hydraulic head gradients and aquifer thickness. The values ρ_f and ρ_s were set to 1000 and 1023 $kg\ m^{-3}$, respectively (Stuyfzand, 1993).

The possible range (uncertainty) in the values of Q , H , c , and k could not be determined from literature. Therefore, the values in Table 2 and the resulting lengths of the offshore tongue of fresh groundwater L are first-order estimates, with the intention to infer the relative differences in L between the five hydrogeological cross-sections. A sensitivity analysis based on a separate increase and decrease (10%) of each of the variables Q , H , c , and k showed that the hydraulic resistance of the semi-confining layer c has the largest influence on the calculated length of the freshwater tongue.

3. Results

3.1. CPT measurements

The lithology and resistivity of the groundwater (ρ_w) inferred from the CPTs are shown for each of the five MLs in Fig. 6. Aquifers and aquitards are also indicated (using AQ n and CL n , respectively, with n being the number of aquifer or confining layer, top down), based on a comparison with the hydrogeological profiles in Fig. 3. The CPT measurements show, with a high vertical resolution, the lithological layering that is present in both the upper, unconfined (AQ1) and the lower confined (AQ2) aquifer. In the confined aquifer (AQ2) thin layers of low permeability are present at MLs 67, 73, 91, and 94. In CPT 94H, a rather thick (~5 m) layer of low permeability is found starting at -19 m NAP. This layer is presumably part of the low-permeable unit that is present in the hydrogeological cross section 94 (Fig. 3) at about -20 m NAP.

The highest CPTs (indicated with 'H'), except for CPT 91H, were taken well above the zone where seawater infiltrates under normal tidal (no-storm) conditions (Table 1 and Fig. 6). The unsaturated zone in these profiles can be identified based on the high resistivities, with $\rho_w \gg 20\ \Omega m$. Below the water table ρ_w shows considerable variations. These variations can be caused by lithological changes (change of the formation factor F), but are more likely due to variations in salinity. The saline groundwater may originate

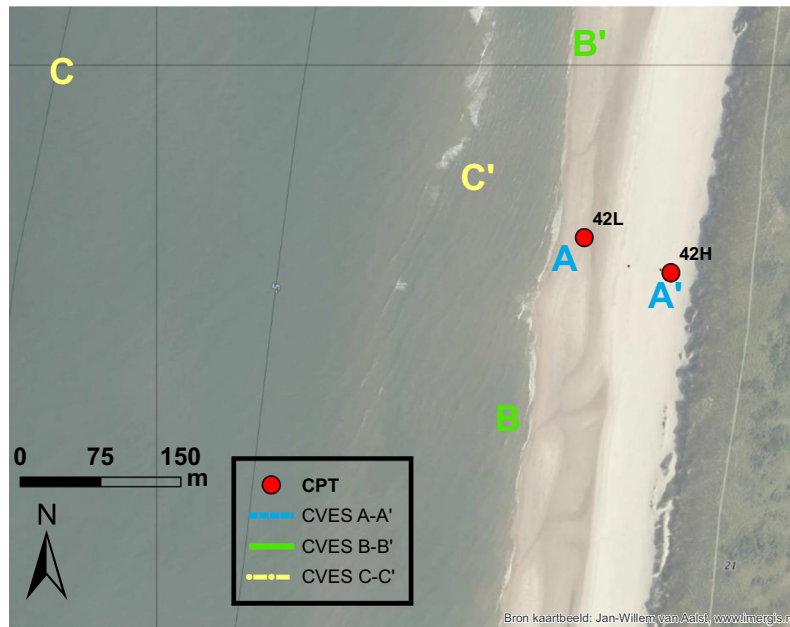


Fig. 5. Location of the CVES measurements and CPTs around ML 42.

Table 2

Q , H , c , k , and calculated L at the five hydrogeological cross-sections. Note that for 'Case II flow' (see [Electronic Supplement](#)) the computed value for L includes the section from the toe of the saltwater wedge to the shore (d/λ in [Bakker \(2006\)](#)).

Hydrogeological cross-section	Q ($\text{m}^2 \text{d}^{-1}$)	H (m)	c (d)	k (m d^{-1})	L (m)
42	0.6	20	500	15	1198
67	0.64	40	200*	30	844
73	0.35	40	150*	30	605
91	0.84	45	200	15	733
94	0.86	30	200	15	739

* The resistance of the confining layer c (CL1; see [Fig. 3](#)) at hydrogeological cross-sections 67 and 73 was deduced from the measured thickness of the freshwater zone below the confining layer at the land-ocean boundary.

from seaspray ([Stuyfzand, 1993](#)) or from the intrusion of seawater during storm surges when the beach floods up to the foot of the dunes. All CPTs taken on the high part of the beach show thick sections of fresh groundwater. These are related to the flow of fresh groundwater from the dune area in the offshore direction.

Because all CPTs at the lower part of the beach (indicated by 'L') are in the area that always inundates during high tide, the measured values of ρ_w in the upper unconfined aquifer are higher than in the higher elevated CPTs at all MLs. In CPT 67L, 73L, and 91L, the entire unconfined aquifer is filled with saline groundwater ($\rho_w < 5 \Omega\text{m}$). In CPTs 42L and 94L, fresh groundwater is found below saline groundwater in the lower part of the unconfined aquifer. The change of ρ_w with depth from the saline to the fresh groundwater is relatively high, and is associated with a thin (\sim i.e. on the order of decimetres) low-permeable layer. In CPTs 67L and 73L there is a clear anomaly in ρ_w between -15 m NAP and -17 m NAP. It is related to lithology as the f_s and q_c values show a concomitant anomaly (see [Electronic Supplement](#)), even though these layers were not classified as low-permeable based on the R_f and du/dz criteria.

The lower CPTs 67L, 73L, and 91L show that the confining layer CL1 is associated with a change in salinity from saline to fresh groundwater. The CPTs at 73L and 67L were deep enough to reach the transition from fresh to saline groundwater in the deeper part of the confined aquifer, revealing the thickness of the freshwater lens here. At the other MLs, the vertical extent of the fresh groundwater could not be constrained as the location of the transition zone was below the maximum depth of the CPTs.

3.2. CVES measurements

The results of the CVES measurements at ML 42 are shown in [Fig. 7](#). The shore-perpendicular CVES measurement A-A' shows the presence of fresh groundwater (high ρ_b) below saline groundwater (low ρ_b). Near the dune-foot (A'), no saline groundwater above fresh groundwater is present because this area is inundated by seawater only occasionally during storms. Towards the lower part of the intertidal area (nearer to A'), the depth of the transition zone between saline and fresh groundwater appears to be increasing. In the shore-parallel CVES measurement B-B' it can be seen that the fresh groundwater extends up to at least 60 m below ground level (bgl), and that it has a shore-parallel extent of at least 100 m (i.e., from $x = 150$ m to $x = 250$ m). Moreover, there is little variation in the thickness of the saltwater layer. The ground level at CVES transects A-A' and B-B' varies between -1 and $+1.5$ m NAP.

The marine CVES measurement C-C' indicates that the fresh groundwater is also present offshore. The decrease of the depth of the ρ_b contours between 0–50 m and 300–400 m are most likely artefacts of the inversion model or caused by an inaccurate incorporation of the bathymetry (thickness and topography of in the seabed). In the [Electronic Supplement](#), different inversion results of C-C' are shown, each with a different bathymetry. It can be seen that the resistivity distribution is highly influenced by the bathymetry. Nevertheless, all tested inversion models reveal fresh groundwater below saline groundwater along the total length of

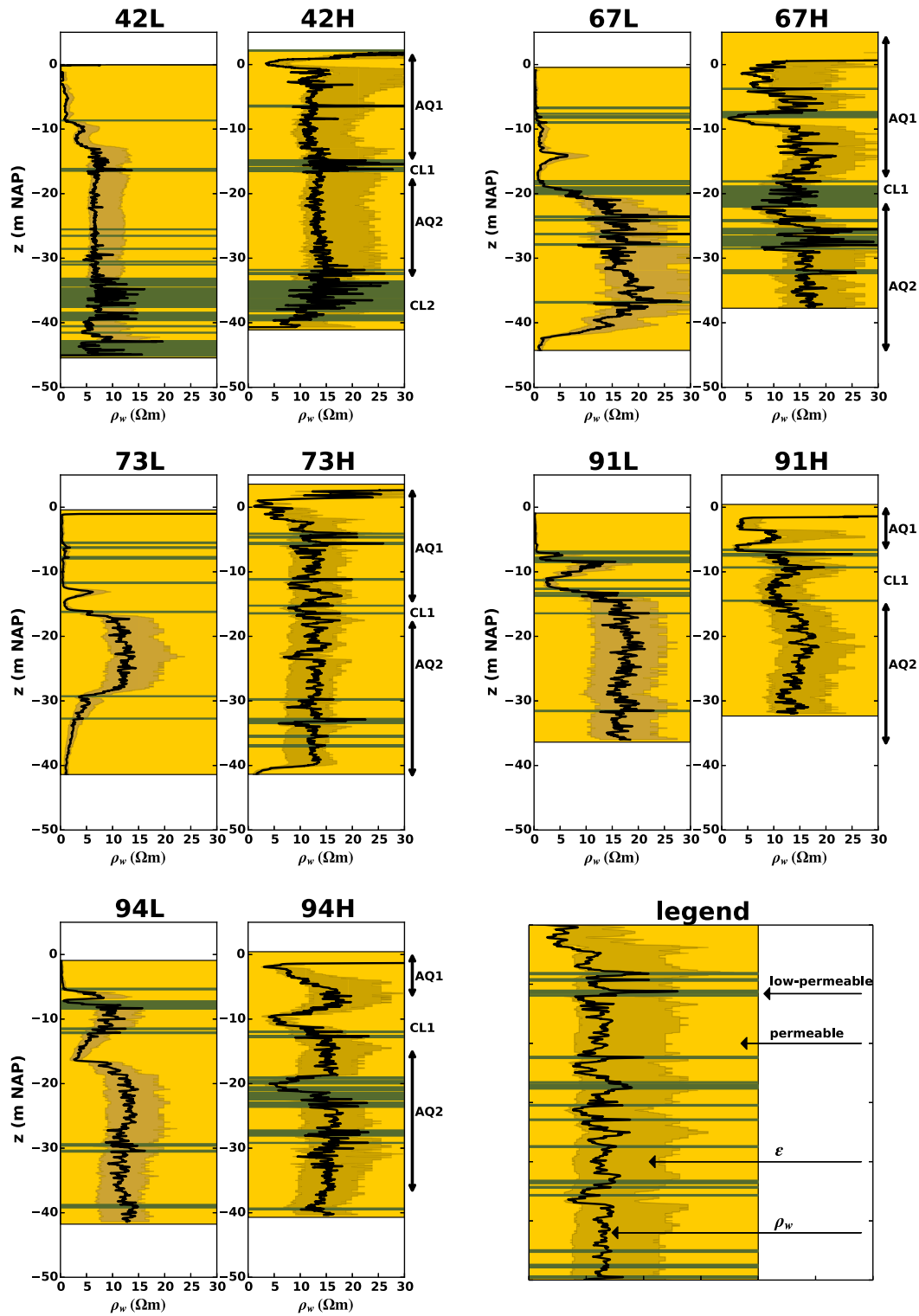


Fig. 6. Graphs showing the results of the CPTs at the five MLs. Labels 'L' and 'H' indicate the CPT taken at the lower part and higher part of the beach, respectively. The values on the vertical axis correspond to the elevation relative to NAP. The black line indicates the calculated water resistivity ρ_w , the shaded grey area indicates the uncertainty (ϵ) of ρ_w associated with the formation factor F . Permeable sections are shown in yellow, low-permeable layers with green lines. On the right of each graph, the interpretation of the aquifers and confining layers (AQ n and CL n , with n being the number of aquifer or confining layer, top down) is indicated. (For interpretation of the references to colour in this figure legend, the reader is referred to the web version of this article.)

the CVES transect C-C' up to a depth of 60 m below NAP below sea level (bsl).

3.3. Analytical calculations of the length of the freshwater tongues in the confined aquifer

The results of the calculations using the equations of Bakker (2006) and the data of Table 2 are shown in Fig. 8. The largest esti-

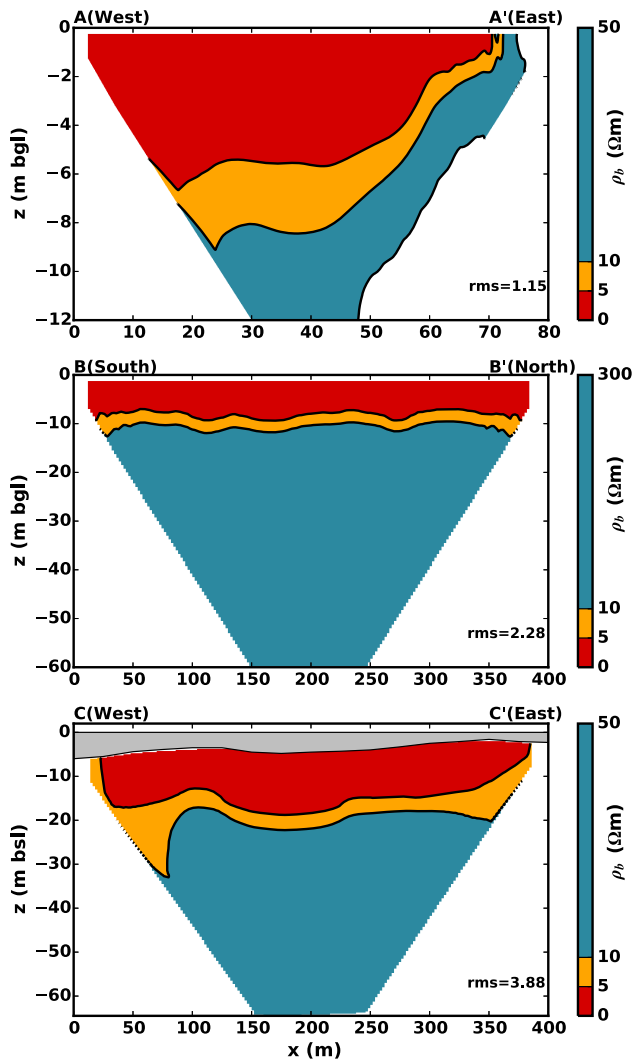


Fig. 7. Results of the inversion of the three CVES measurements. x denotes the distance along the profile. In CVES A-A' and B-B' the depth z is shown below ground level (bgl); in CVES C-C' the depth is shown below sea level (bsl). Both bgl and bsl are within 1.5 m from NAP. In CVES C-C', the seawater (incorporated in the inversion model) is shown in grey. On the lower right in each subfigure, the root mean square error (rms; based on the difference between the measured and calculated apparent resistivity) of the inversion models is shown. Note that the upper subfigure (CVES A-A') is at a different scale than the ones below.

mated length of the freshwater tongue relative to the coastline (L) was calculated for hydrogeological cross-section 42, the smallest for 73 (Table 2). The reasons that L is highest at cross-section 42 is that both the hydraulic resistance of the confining layer and the groundwater flow rate are high compared to the other cross-sections. Although L in cross-sections 67, 73, 91 and 94 is comparable, the length of the wedge of intruded seawater inland of the coastline varies. The calculated intrusion lengths are consistent with the hydrogeological cross-sections shown in Fig. 3.

4. Discussion

4.1. Unconfined aquifer

Previous field and modelling studies on submarine groundwater discharge from shallow unconfined aquifers have described a saline groundwater circulation cell below the beach and a distinct 'tube' a fresh groundwater discharging at the lower part of the

intertidal area (Vandenbohede and Lebbe, 2005; Robinson et al., 2007). The presence of a tube of fresh groundwater above the first low-permeability layer encountered, would be manifest in the CPTs taken at the lower part of the intertidal zone as a layer with a high bulk resistivity (or calculated groundwater resistivity) below a layer, presumably a few meters thick, with a low resistivity. However, this was the case in none of the CPTs, as all groundwater above the first low-permeability layer was classified as 'saline'. It could therefore not be ascertained if the transition from shallow saline- to deeper freshwater is sustained by active circulation driven by tides, as found in aforementioned studies elsewhere, or if it is the result of different processes.

The interpretation of the CPTs regarding the salinity distribution in the unconfined aquifer is schematically shown in Fig. 9. At the higher part of the beach (i.e., around or landward of the highest astronomical tide mark) fresh groundwater is found over a large depth of the unconfined aquifer, indicating the flow of fresh groundwater towards the sea. Note that for simplification the variations of ρ_w indicated by the CPTs at the higher part of the beach have been omitted from Fig. 9. Around the lowest astronomical tide mark,

ML 67, 73, and 94 have saline groundwater over the entire thickness of the unconfined aquifer. This does not imply that this is pure seawater, but the adopted classification masks any variability within the saltwater that may result from mixing. Only in CPTs 42L and 94L fresh groundwater was found below saline groundwater in the unconfined aquifer, but this was associated with a low-permeable layer. If a distinct outflow zone of (relatively) fresh groundwater is present at these locations, it is expected to be further offshore instead of near the low water line. A conceptual model showing the inferred salinity distribution below the beach for both the case with (solid colors) and without a low-permeable layer (dotted line) within the unconfined aquifer is shown in Fig. 9. A more sophisticated experimental design is required though to elucidate the flow processes in the unconfined aquifer in our study area. In any case, the CPT measurements highlight that the lithological variability at a short vertical scale exerts a strong control on the groundwater salinity.

4.2. Confined aquifer(s)

At all five hydrogeological cross-sections, fresh groundwater was confirmed in the confined aquifer below the beach. Hence, it is likely that at each location the fresh dune groundwater flow system extends a certain distance offshore, which was estimated for each location based on the equations by Bakker (2006). The results are included in Table 2 and Fig. 8, and should be treated as a first-order assessment because of the strict assumptions contained in the analytical expressions, which become particularly questionable when the freshwater flux and the hydraulic resistance of the confining layer are low (Kooi and Groen, 2001). For example, assuming a uniform resistance of the semi-confining layer c in the equations of Bakker (2006) is questionable, as the CPTs indicate that the low-permeable layers comprising the semi-confining layer show spatial variability across the relatively small scale of the beach extent.

Historic offshore hydrochemical data suggest a greater offshore extent than inferred from the analytical equations. In 1964 a borehole was drilled about 2 km offshore in the harbour of the city IJmuiden (Fig. 2) and groundwater samples were taken down to a depth of -52 m NAP (Stuyfzand, 1987b). The water resistivity (ρ_w , inferred from the measured electrical conductivity) of the samples showed that the groundwater below the confining layer was considerable less saline than the overlying seawater (Fig. 10). Whilst the flow conditions at this location were comparable to the other MLs in the past, the seaward flow of fresh groundwater from the dunes became considerably reduced at the end of

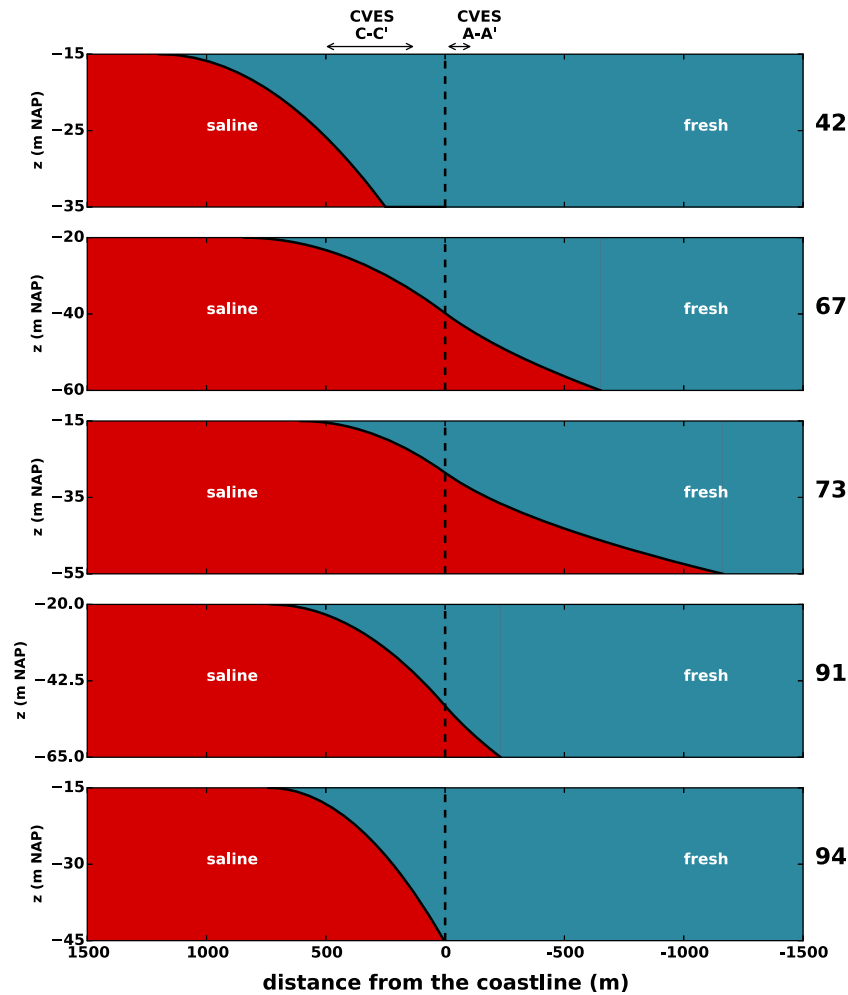


Fig. 8. Cross sections showing the calculated configuration of the offshore tongues of fresh groundwater. The locations of the marine CVES C-C' and the shore-perpendicular CVES A-A' at the beach are also indicated. The dashed line at $x = 0$ represents the sharp land-ocean boundary. Negative values of x are onshore, positive values of x are offshore.

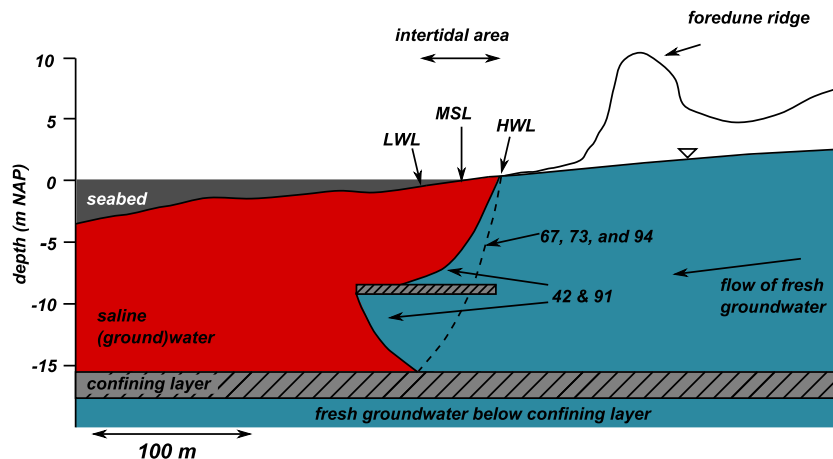


Fig. 9. Simplified interpretation of the salinity distribution below the beach at the different MLs. HWL and LWL are the highest and lowest astronomical tide marks, respectively. The solid colors indicate the situation with the presence of a low-permeable layer in the unconfined aquifer, the dotted line indicates the situation when such a layer is absent. (For interpretation of the references to colour in this figure legend, the reader is referred to the web version of this article.)

the 19th century when a harbour and a canal were built by excavating the dunes, deflecting the groundwater flow towards the north. The salinities measured in 1964 were therefore most likely higher than what they would have been when there was more freshwater flow under the seabed. Cation concentration data (not

shown) of the samples between -27 and -52 m NAP show that the groundwater is currently experiencing salinization (Stuyfzand, 1987b, 1993), which is consistent with a shrinking body of offshore freshwater.

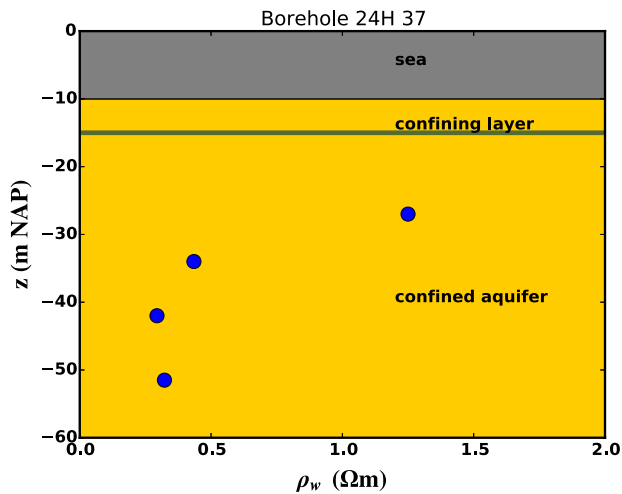


Fig. 10. Results of the groundwater resistivity ρ_w of the groundwater sampling at four different depths in borehole 24H 37, located about 2 km offshore in harbour of the city IJmuiden. The blue dots indicate the depths at which a groundwater sample was taken (except for the upper one, which was taken in the sea). Grey indicates the sea, yellow an aquifer (sandy sediment) and green a confining layer. (For interpretation of the references to colour in this figure legend, the reader is referred to the web version of this article.)

An important process that was neglected in the application of the equations of Bakker (2006) is the historical development of the coastline. Since 1990, the coastline has remained stable due to beach and near-shore sand nourishments. Before 1990, over the past centuries, parts of the coastline have been subjected to structural marine erosion, leading to an important landward migration of the coastline. For example, near the city of Egmond, about 5 km north of ML42, the coastline has moved about 300 m inland since the 16th century (Stuyfzand, 1985). Such a coastline migration has certainly influenced the dune groundwater flow system. Due to the long response time of freshwater lenses in confined aquifer systems to changing hydraulic boundary conditions, it may well be that the offshore occurrences of freshwater are relics of the freshwater lens that existed under former dune landscapes that extended further to the west. Other important reasons for freshwater lenses (including their offshore extension) not being in steady state are the historic groundwater extraction and the artificial infiltration in the dune area. Conclusions about the transience of the fresh groundwater flow system extending offshore cannot be drawn from the geophysical data. Numerical modelling remains intractable until the geology beneath the seafloor is better characterised, which requires, for example, seismic surveys. Therefore, repeated geophysical monitoring or hydrochemical and isotope data obtained by offshore drilling are a better alternative to investigate how the freshwater body is responding to changing boundary conditions.

4.3. Practical aspects of CPT measurements for coastal hydrology

Among the advantages of the CPT method over drilling are the less complicated logistics (as no drilling mud or casings are required), lower costs involved, and a faster operation time. The latter advantage is especially important when working in the intertidal area. A single CPT up to a depth of over 40 m was found lasts up to circa 2 h at the sites investigated, which means it could be completed during falling tide (6 h). Because no chemicals are used, and the equipment makes less noise than conventional drill rigs, there is also a wider scope for application of the method in ecologically-sensitive area along the coast.

The CPT does not yield direct measurements of the groundwater salinity. Methods to retrieve groundwater samples during a CPT can help to distinguish the lithology and groundwater salinity from the measured bulk electrical resistivity. The probe can be equipped with dedicated sampling chambers, or well screens can be placed after the CPT measurement using a sacrificial cone tip. Although more costly and leading to a longer operation time, such methods are available. Direct sampling also provides an opportunity for more comprehensive analysis of the chemical and isotopic composition of the groundwater. For the offshore region, the CPT truck could be mounted on a platform.

5. Conclusions

In coastal aquifers the offshore directed flow of fresh groundwater results in discharge and mixing with saline groundwater or surface water. This can take place in the unconfined aquifer as well as in the underlying confined aquifer(s). Although at the shoreline fresh groundwater can flow simultaneously in both systems, most of the existing field-based studies have focused on superficial unconfined systems. This paper presents the results of an investigation of the salinity patterns in both the unconfined aquifer and confined aquifer along the coast of the Western Netherlands. Existing hydrogeological and new geophysical data were compiled for five shore-normal cross-sections, extending from the beach to 4 km inland. The presence of freshwater below the beach was established using cone penetration tests, and the likely offshore continuation of fresh groundwater flow was assessed using analytical models.

Freshwater was only found in the unconfined aquifer below intercalations of low-permeable layers, which separate it from more saline water above. Fresh groundwater in the confined aquifer at the shoreline was confirmed by the CPTs at all measurement locations, and is expected to continue at least a few hundred meters below the seabed. It is unclear if the offshore extent of the freshwater lens is due to the active sub-sea flow of groundwater or if the lower salinities offshore represent relic conditions of a more westerly (seaward) located shoreline. There remains a need for targeted sampling of groundwater in the offshore realm to resolve this.

The CPT data were found to be a valuable complement to the existing data that were based on traditional hydrogeological methods. It is expected that the technique can be used in other studies of beach hydrology to effectively establish the relationship between salinity and lithology. More comprehensive experimental designs, that combine CPTs equipped with direct samplers with a suite of other hydrogeological and hydrochemical characterisation techniques, have great potential to further increase our understanding of both shallow and deeper beach and offshore groundwater dynamics.

Acknowledgements

Frans Backer (VU Amsterdam) is thanked for collecting the CVES field data of profiles B-B' and C-C'. We acknowledge the financial and data contributions of the water supply companies Dunea, Waternet, and PWN that made this research possible.

Appendix A. Supplementary data

Supplementary data associated with this article can be found, in the online version, at <http://dx.doi.org/10.1016/j.jhydrol.2017.04.021>.

References

- Abarca, E., Karam, H., Hemond, H.F., Harvey, C.F., 2013. Transient groundwater dynamics in a coastal aquifer: the effects of tides, the lunar cycle, and the beach profile. *Water Resour. Res.* 49 (5), 2473–2488.
- Andersen, M.S., Baron, L., Gudbjerg, J., Gregersen, J., Chapellier, D., Jakobsen, R., Postma, D., 2007. Discharge of nitrate-containing groundwater into a coastal marine environment. *J. Hydrol.* 336 (1–2), 98–114. <http://dx.doi.org/10.1016/j.jhydrol.2006.12.023>.
- Archie, G.E., 1942. The electrical resistivity log as an aid in determining some reservoir characteristics. *Trans. AIME* 146, 54–62.
- Bakker, M., 2006. Analytic solutions for interface flow in combined confined and semi-confined, coastal aquifers. *Adv. Water Res.* 29 (3), 417–425. <http://dx.doi.org/10.1016/j.advwatres.2005.05.009>.
- Bakker, M., Schaars F., 2006. How to become a Jedi master in modeling seawater intrusion with MODFLOW-SWI. In: Proc. 21st Salt Water Intrusion Meeting. Azores, Portugal. pp. 317–320.
- Bear, J., Cheng, A.-H., Sorek, S., Ouazar, D., Herrera, I., 1999. *Seawater Intrusion in Coastal Aquifers Concepts, Methods and Practices*. Springer, Berlin. 640 pp.
- Custodio, E., Bruggeman, G.A., 1987. Groundwater problems in coastal areas: a contribution to the International Hydrological Programme. Studies and reports in hydrology. vol. 45. Paris.
- Dufour, D.C., 1998. *Grondwater In Nederland: Onzichtbaar Water Waarop Wij Lopen*. TNO, Delft, ISBN 90-6743-536-8.
- Greskowiak, J., 2014. Tide-induced salt-fingering flow during submarine groundwater discharge. *Geophys. Res. Lett.* 41, 6413–6419. <http://dx.doi.org/10.1002/2014GL061184>.
- Hayashi, M., 2003. Temperature-electrical conductivity relation of water for environmental and geophysical data inversion. *Environ. Monit. Assess.* 96, 119–128.
- Kooi, H., Groen, J., 2001. Offshore continuation of coastal groundwater systems; predictions using sharp-interface approximations and variable-density flow modelling. *J. Hydrol.* 246 (1–4), 19–35. [http://dx.doi.org/10.1016/S0022-1694\(01\)00354-7](http://dx.doi.org/10.1016/S0022-1694(01)00354-7).
- Krantz, D.E., Manheim, F.T., Bratton, J.F., Phelan, D.J., 2004. Hydrogeologic setting and ground water flow beneath a section of Indian River Bay, Delaware. *Ground Water* 42 (7), 1035–1051. <http://dx.doi.org/10.1111/j.1745-6584.2004.tb02642.x>.
- Lebbe, L., 1983. Mathematical model of the evolution of the fresh water lens under the dunes and beach with semi-diurnal tides. 8th Salt Water Intrusion Meeting, Bari. *Geologia Applicata e Idrogeologia*, volume XVIII, parte II, 211–226.
- Loke, M.H., 2006. RES2DINV ver. 3.55, Rapid 2-D resistivity & IP inversion using the least-squares method, 139 pp., Geotomo Software, Penang, Malaysia.
- Lunne, T., Robertson, P.K., Powell, J.J.M., 1997. Cone penetration testing in geotechnical practice. Blackie Academic & Professional, 312 pp.
- Michael, H.A., Mulligan, A.E., Harvey, C.F., 2005. Seasonal oscillations in water exchange between aquifer and the coastal ocean. *Nature* 436 (7054), 1145–1148.
- Moore, W.S., 2010. The effect of submarine groundwater discharge on the ocean. *Ann. Rev. Marine Sci.* 2, 59–88. <http://dx.doi.org/10.1146/annurev-marine-120308-081019>.
- Mulligan, A., Charette, M., 2006. Intercomparison of submarine groundwater discharge estimates from a sandy unconfined aquifer. *J. Hydrol.* 327 (3–4), 411–425. <http://dx.doi.org/10.1016/j.jhydrol.2005.11.056>.
- Mulligan, A.E., Evans, R., Lizarralde, D., 2007. The role of paleochannels in groundwater/seawater exchange. *J. Hydrol.* 335 (3–4), 313–329. <http://dx.doi.org/10.1016/j.jhydrol.2006.11.025>.
- Revil, A., Karaoulis, M., Johnson, T., Kemna, A., 2012. Some low-frequency electrical methods for subsurface characterization and monitoring in hydrogeology. *Hydrogeol. J.* 20, 617–658.
- Robinson, C., Li, L., Barry, D.A., 2007. Effect of tidal forcing on a subterranean estuary. *Adv. Water Res.* 30 (4), 851–865. <http://dx.doi.org/10.1016/j.advwatres.2006.07.006>.
- Stuyfzand, P.J., 1985. Hydrochemie en hydrologie van het duingebied tussen Egmond en Wijk aan Zee (Hydrochemistry and hydrology of the coastal dune area between Egmond and Wijk aan Zee). KIWA rep. SWE-85.012.
- Stuyfzand, P.J., 1987. Hydrochemie en hydrologie van duinen en aangrenzende polders tussen Noordwijk en Zandvoort aan Zee (Hydrochemistry and hydrology of the coastal dune area and adjacent polders between Noordwijk and Zandvoort aan Zee). KIWA rep. SWE-87.007.
- Stuyfzand, P.J., 1987. Hydrochemie en hydrologie van duinen en aangrenzende polders tussen Zandvoort en Wijk aan Zee (Hydrochemistry and hydrology of the coastal dune area and adjacent polders between Zandvoort en Wijk aan Zee). KIWA rep. SWE-86.016.
- Stuyfzand, P.J., 1993. Hydrochemistry and hydrology of the coastal dune area of the Western Netherlands (Ph.D. thesis). Vrije Univ. Amsterdam, Published by KIWA, 366 pp.
- Stuyfzand, P.J., 2016. Observations and analytical modeling of freshwater and rainwater lenses in coastal dune systems. *J. Coastal Conservation*. <http://dx.doi.org/10.1007/s11852-016-0456-6>. September 1–17. <http://www.readcube.com/articles/10.1007/s11852-016-0456-6?author_access_token=AcJmBHPfVWRqjV_CT2bOYPe4RwlQNchNByi7wbcMAY50t6C33h75P0jn00LQsGw_hhH58yY8YNJ88GeTQC1mfzoPLmx7aogBv9sC_AF8Fb5FCm1YwCj7JpsbA8f5OabdPUfHei-r3MN1PufQz_fcw%3D%3D>.
- Stuyfzand, P.J., Lüers, F., De Jonge, H.G., 1993. Hydrochemie en hydrologie van duinen en aangrenzende polders tussen Katwijk en Kijkduin. KIWA rep. SWE-93.001.
- Taniguchi, M., Burnett, W.C., Cable, J.E., Turner, J.V., 2002. Investigation of submarine groundwater discharge. *Hydrol. Process.* 16, 2115–2119.
- Van den Helder, M., 2011. Modelleren overgang zoet-zout grondwater met SEAWAT in Het Nieuwe Water, Waterkamer 4 (M.Sc. thesis), Fac. of Earth Life Sciences, Vrije Univ. Amsterdam.
- Vandenbohede, A., Lebbe, L., 2005. Occurrence of salt water above fresh water in dynamic equilibrium in a coastal groundwater flow system near De Panne, Belgium. *Hydrogeol. J.* 14 (4), 462–472. <http://dx.doi.org/10.1007/s10040-005-0446-5>.
- Walter, F., 1976. Geofysisch onderzoek ter bepaling van bodemconstanten. In: De winning en aanvulling van grondwater en beïnvloeding van de omgeving. Technische Hogeschool Delft, Afd. Weg- en Waterbouwkunde.
- Waxman, M.H., Smits, L.J.M., 1968. Electrical conductivities in oil-bearing shaly sands. *Soc. Pet. Eng. J.* 8 (2), 107–122. <http://dx.doi.org/10.2118/1863-A>.
- Werner, A.D., Bakker, M., Post, V.E.A., Vandenbohede, A., Lu, C., Ataie-Ashtiani, B., Simmons, C.T., 2013. Seawater intrusion processes, investigation and management: recent advances and future challenges. *Adv. Water Res.* 51, 3–26. <http://dx.doi.org/10.1016/j.advwatres.2012.03.004>.